

DRAFT TRIB2004-64015

A COMPACT MODEL FOR SPHERICAL ROUGH CONTACTS

M. Bahrami¹, M. M. Yovanovich², and J. R. Culham³

Microelectronics Heat Transfer Laboratory,
Department of Mechanical Engineering,
University of Waterloo, Waterloo, ON, Canada N2L 3G1

Abstract

The contact of rough spheres is of high interest in many tribological, thermal, and electrical fundamental analyses. Implementing the existing models is complex and requires iterative numerical solutions. In this paper a new model is presented and a general pressure distribution is proposed that encompasses the entire range of spherical rough contacts including the Hertzian limit. It is shown that the non-dimensional maximum contact pressure is the key parameter that controls the solution. Compact expressions are proposed for calculating the pressure distribution, radius of the contact area, elastic bulk deformation, and the compliance as functions of the governing non-dimensional parameters. The present model shows the same trends as those of the Greenwood and Tripp model. Correlations proposed for the contact radius and the compliance are compared with experimental data collected by others and good agreement is observed.

NOMENCLATURE

A	=	area, m^2
a	=	radius of contact, m
a'_L	=	relative contact radius, $\equiv a_L/a_H$
d_v	=	Vickers indentation diagonal, m
E	=	Young's modulus, Pa
E'	=	equivalent elastic modulus, Pa
F	=	external force, N
H	=	hardness, Pa
H_{mic}	=	microhardness, Pa

m	=	mean absolute asperity slope
n_s	=	number of microcontacts
P	=	pressure, Pa
P'_0	=	relative max pressure, $\equiv P_0/P_{0,H}$
r	=	radial position, m
Y	=	separation between mean planes, m

Greek

α	=	roughness parameter, $\equiv \sigma\rho/a_H^2$
β	=	radius of summits, m
γ	=	exponent of general pressure distribution
η	=	summits density, m^{-2}
κ	=	compliance, m
λ	=	non-dimensional separation, $\equiv Y/\sqrt{2}\sigma$
μ	=	non-dimensional parameter, $\equiv 8\sigma\eta\sqrt{2\rho\beta}/3$
ν	=	Poisson's ratio
ξ	=	non-dimensional radial position, $\equiv r/a_L$
ρ	=	radius of curvature, m
σ	=	RMS surface roughness, μm
τ	=	non-dimensional parameter, $\equiv \rho/a_H$
ω	=	deformation, m

Subscripts

0	=	value at origin
1	=	surface 1
2	=	surface 2
a	=	apparent, asperity
b	=	bulk
H	=	Hertz
L	=	large
r	=	real
s	=	small, summit
v	=	Vickers

¹Ph.D. Candidate, Department of Mechanical Engineering.

²Distinguished Professor Emeritus, Department of Mechanical Engineering. Fellow ASME.

³Associate Professor, Director, Microelectronics Heat Transfer Laboratory. Member ASME.

INTRODUCTION

Hertzian theory of contact between elastic bodies is based on the assumption that the contacting surfaces are ideally smooth and thus perfect contact takes place throughout the nominal contact area. However, real surfaces have roughness and contact occurs only at discrete spots called microcontacts, where asperities make contact. The real contact area is usually a small fraction of nominal contact area. Therefore, Hertzian contact is a limiting case where surfaces are considered ideally smooth. Spherical rough contact analysis includes two problems at different scales, i) the bulk or macroscale compression and ii) deformation of asperities.

The contact area is the area where the microcontacts are distributed; also the contact pressure falls off to a negligible value (zero in the Hertz limit) at the edge of the contact area. Hertz replaced the contacting spherical surfaces with paraboloids; thus the contact between two spheres was simplified to the contact of a plane and a sphere that has an effective radius ρ , where $1/\rho = 1/\rho_1 + 1/\rho_2$. For convenience, all elastic deformations can be considered to occur in one body, which has an effective elastic modulus E' , and the other body is assumed to be rigid. The effective elastic modulus can be found from

$$\frac{1}{E'} = \frac{1 - \nu_1^2}{E_1} + \frac{1 - \nu_2^2}{E_2} \quad (1)$$

Hertz also assumed a contact pressure distribution in the form of

$$P_H(r/a_H) = P_{0,H} \sqrt{1 - (r/a_H)^2} \quad (2)$$

where $P_{0,H} = 1.5F/(\pi a_H^2)$ and $a_H = (0.75F\rho/E')^{1/3}$ are the maximum pressure and the radius of the Hertzian contact area, respectively.

A common methodology to model the roughness is the representation of the asperities by simple geometrical shapes with a probability distribution for the different asperity parameters involved. If the asperities of a surface are isotropic and randomly distributed, the surface is called Gaussian. Williamson et al. [1] have shown experimentally that many of the techniques used to produce engineering surfaces give a Gaussian distribution of surface heights. The contact between Gaussian rough surfaces is modeled by the contact between a single Gaussian surface that has the effective surface characteristics with a perfectly smooth surface. The equivalent roughness σ and asperity slope m can be found from $\sigma = \sqrt{\sigma_1^2 + \sigma_2^2}$ and $m = \sqrt{m_1^2 + m_2^2}$, respectively.

Different approaches can be taken to analyze the deformation of asperities by assuming plastic [2], elastic [3], or elastoplastic [4, 5] regimes at microcontacts. It was observed through experiments that the real contact area is

proportional to the load [6, 7]. However, if elastic deformation is assumed, using Hertzian theory, the real contact area will not be linearly proportional to the load, $A_r \propto F^{2/3}$. Archard [8] solved this problem by assuming that the surface asperities have micro-asperities and micro-asperities have micro-micro asperities and so on, by adding several levels of asperities, it can be shown that $A_r \propto F$. Greenwood and Williamson (GW) [3] subsequently developed an elastic contact model that has been widely accepted, they proposed that as the load increases new microcontacts are nucleated while the mean size of microcontacts remains constant. The main assumptions of the GW model are i) asperity heights have a Gaussian distribution; the distribution of summit heights is the same as the surface heights standard deviation, i.e., $\sigma_s = \sigma$, ii) asperity summits have a spherical shape all with a constant radius β , and iii) asperities entirely deform elastically, i.e., Hertzian theory can be applied for each individual summit. According to the GW model, the summits or “peaks” on a surface profile are the points higher than their immediate neighbors at the sampling interval used. Recently Greenwood and Wu [9] reviewed the assumptions of the GW model and concluded that “the GW definition of peaks is wrong and gives a false idea of both number and the radius of curvature of asperities”. Greenwood and Wu proposed to return to the Archard idea that roughness consists of roughness on roughness and that the contact may be plastic at light loads but it becomes elastic at heavier loads.

Considering an indentation hardness for asperities, Persson [10] concluded, as GW did, that except for polished surfaces all microcontacts deform plastically. Later, it will be shown that the deformation mode of asperities has a second order effect on spherical rough contacts and both elastic and plastic models give similar results.

LITERATURE REVIEW

The open literature contains very few analytical models for the contact of spherical rough surfaces. The first in-depth analytical study to investigate the effect of roughness on elastic spherical bodies was performed by Greenwood and Tripp (GT) [11]. The GT model was developed based on the same assumptions as the GW model for microcontacts. Moreover, the bulk deformation was assumed to be elastic. The elastic deformation produced by an arbitrary pressure distribution over a circular area on a half-space can

be found from [11, 12]

$$\omega_b(r) = \begin{cases} \frac{2}{E'} \int_0^a P(s) ds & r = 0 \\ \frac{4}{\pi E' r} \int_0^r s P(s) K\left(\frac{s}{r}\right) ds & r > s \\ \frac{4}{\pi E'} \int_r^\infty P(s) K\left(\frac{r}{s}\right) ds & r < s \end{cases} \quad (3)$$

where $K(\cdot)$ is the complete elliptic integral of the first kind and a is the radius of the circle. Greenwood and Tripp [11] reported a complete set of relationships and solved it numerically. The results of the GT analysis were found to be primarily a function of a non-dimensional parameter $T = 2F/\sigma E' \sqrt{2\rho\sigma}$ and a weak function of $\mu = 8\sigma\eta\sqrt{2\rho\beta}/3$. The most important trends in the GT model were that an increase in roughness resulted in a decrease in the pressure and an increase in the contact area. The GT model was a significant achievement, however its limitations are,

- the GT model was presented as a set of relationships; applying the model is complex and requires numerically intensive solutions
- two of its input parameters, i.e., summits radius β and density η cannot be measured directly and must be estimated through statistical calculations. Additionally, these parameters are sensitive to the surface measurements [7, 9].

Roca and Mikic [13] developed an alternative numerical model by assuming plastic deformation of asperities and that the height of the surface roughness has a Gaussian distribution. Similar trends to those of the GT model were presented. The modeling results of [13] was also mainly a function of a non-dimensional parameter $\bar{\sigma} = \pi\sigma E'/a_H P_{0,H}$ and a weak function of $H/P_{0,H}$, where $P_{0,H}$ is the maximum pressure in the Hertzian limit. Mikic and Roca did not report general relations to calculate the contact parameters.

Greenwood et al. [14] introduced a non-dimensional parameter α called roughness parameter that governs primarily the rough spherical contact as

$$\alpha = \frac{\sigma\rho}{a_H^2} = \sigma \left(\frac{16\rho E'^2}{9F^2} \right)^{1/3} \quad (4)$$

Greenwood et al. [14] showed that the controlling non-dimensional parameters in both [11] and [13] models can be written in terms of α , i.e., $T = 4\sqrt{2}/3\sqrt{\alpha^3}$ and $\bar{\sigma} = 3\pi^2\alpha/4$, respectively. They concluded that it is unimportant whether the asperities deform elastically or plastically; the contact pressure is predominantly governed by α . Further, if the value of α is less than 0.05, the effect of roughness is negligible and the Hertzian theory can be used.

MODEL DEVELOPMENT

In this study, the deformation of asperities is assumed to be plastic. As a result, bringing two rough surfaces together within a distance Y is equivalent to removing the top of the asperities at a height Y above the mean plane. The assumption of pure plastic microcontacts enables the micro mechanics to be specified completely by surfaces roughness σ (rather than the summit heights as in the GT model) and the mean asperity slope m without having to assume some deterministic peak shapes as with elastic models. Cooper et al. [2] modeled surface roughness as hemispherical asperities whose heights and slopes have Gaussian distributions σ and m , respectively. The following summarizes the relationships for the contact of conforming rough surfaces [15]:

$$\begin{aligned} a_s &= \sqrt{\frac{8}{\pi}} \left(\frac{\sigma}{m} \right) \exp(\lambda^2) \operatorname{erfc} \lambda \\ n_s &= \frac{1}{16} \left(\frac{m}{\sigma} \right)^2 \frac{\exp(-2\lambda^2)}{\operatorname{erfc} \lambda} A_a \\ \frac{A_r}{A_a} &= \frac{1}{2} \operatorname{erfc} \lambda \end{aligned} \quad (5)$$

where $\lambda = Y/\sqrt{2}\sigma$ and $\operatorname{erfc}(\cdot)$ is the complementary error function.

Microhardness is not constant throughout the material and in most surfaces is greater than the bulk hardness [10, 15]. It decreases with increasing depth of the indenter until the bulk hardness is obtained. Hegazy [16] proposed empirical correlations to account for the decrease in microhardness with increasing penetration depth in the form of

$$H_v = c_1 (d'_v)^{c_2} \quad (6)$$

where H_v is the Vickers microhardness, $d'_v = d_v/d_0$ and $d_0 = 1 \mu\text{m}$.

In the present model, the bulk deformation is assumed to be elastic. Due to the surface curvature, the separation and consequently the mean size and the number of the microcontacts vary with radial position. The contact area is divided into infinitesimal surface elements, dr , where the conforming rough relationships, Eq. (5) can be applied. In the vicinity of the contact the profile of the sphere can be approximated by a paraboloid, $u(r) = u_0 - r^2/2\rho$. The local separation $Y(r)$ is the distance between two mean planes of the contacting surfaces, Fig. 1, and can be written as

$$Y(r) = \omega_b(r) - u(r) = \omega_b(r) - u_0 + r^2/2\rho \quad (7)$$

A schematic free-body diagram of the contact is shown in Fig. 2. As previously mentioned, all the bulk deformations are assumed to occur in the elastic half space which has an effective elasticity modulus E' . Discrete point forces are created at the microcontacts where the pressure is the

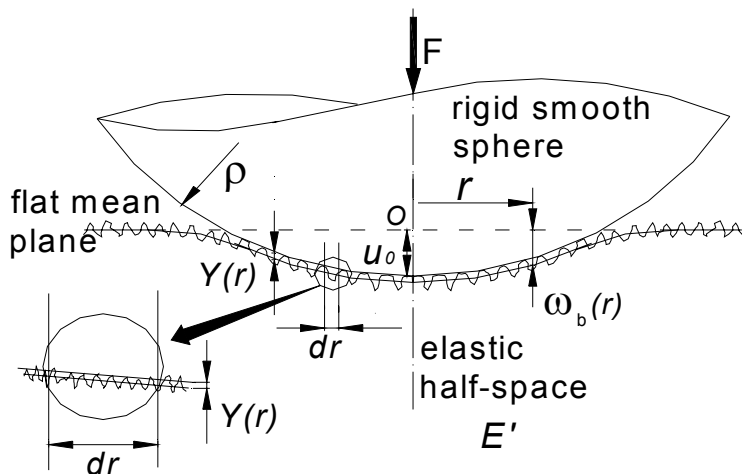


Figure 1. CONTACT BETWEEN SPHERE AND ROUGH PLANE

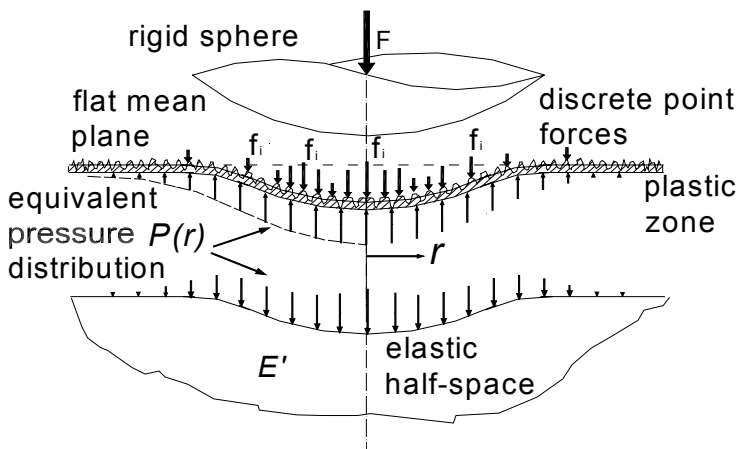


Figure 2. FREE-BODY DIAGRAM OF CONTACT, DISCRETE POINT FORCES AND PLASTIC LAYER

microhardness of the softer material in contact. The surface roughness acts like a plastic zone on an elastic half-space, in the sense that the effect of these point forces on the elastic half-space is considered as a continuous pressure $P(r)$. In a surface element dr , Fig. 1, the local separation $Y(r)$ is uniform. Therefore, the ratio of the real to apparent area can be found from Eq. (5)

$$\frac{dA_r(r)}{dA_a(r)} = \frac{1}{2} \operatorname{erfc} \lambda(r) \quad (8)$$

The local microhardness is determined from the Vickers microhardness correlation, Eq. (6) as a function of the local mean microcontact radius $a_s(r)$. The relation between the

Vickers diagonal d_v and the microcontact radius a_s , based on equal areas, is $d_v = \sqrt{2\pi}a_s$. Therefore, the local microhardness is $H_{mic}(r) = c_1 [\sqrt{2\pi} a_s(r)]^{c_2}$. The local radius $a_s(r)$ and the number of the microcontacts $n_s(r)$ can be found from Eq. (5).

The external load F is the summation of the point forces acting at the microcontacts

$$F = \sum_i f_i = \iint_{\text{contact area}} H_{mic}(r) dA_r(r) \quad (9)$$

Combining Eqs. (8) and (9) and considering a circular contact area, one obtains

$$F = \pi \int_0^\infty H_{mic}(r) \operatorname{erfc} \lambda(r) r dr \quad (10)$$

The upper limit of the integral is set to infinity, since the contact radius, a_L , is not known at this stage. But, it will not effect the final solution because the effective pressure distribution rapidly approaches zero at the edge of the contact area. On the bulk side, the contact pressure must also satisfy the force balance, thus, the pressure distribution can be found from

$$P(r) = \frac{1}{2} H_{mic}(r) \operatorname{erfc} \lambda(r) \quad (11)$$

The elastic displacement of the half-space can be found by substituting the pressure distribution Eq. (11) into Eq. (3). Equations (3), (5), (8), (10), and (11) form a closed set of governing relationships. An algorithm and a computer program were developed to solve the set numerically [17].

Figure 3 shows the effect of roughness on the contact pressure predicted by the model. The program was run for a wide range of roughness (and accordingly asperity slope) while other input parameters shown in Fig. 3 were kept constant. As shown, the contact pressure approaches the Hertzian pressure as the roughness approaches zero. Unlike the Hertzian contact, pressure distributions asymptotically approach zero. As a result, the contact radius is not an exact point and its definition is rather arbitrary. However, in this study, it is considered as the radius where the normalized pressure is negligible, i.e., $P(r = a_L)/P_0 < 0.01$.

GENERAL PRESSURE DISTRIBUTION

The main goal of this study is to develop compact relations for determining compliance, contact pressure, and the contact radius as functions of non-dimensional parameters that describe the contact problem. To reach this goal, the following simplifications are made: i) an effective microhardness H_{mic} is considered which is constant throughout

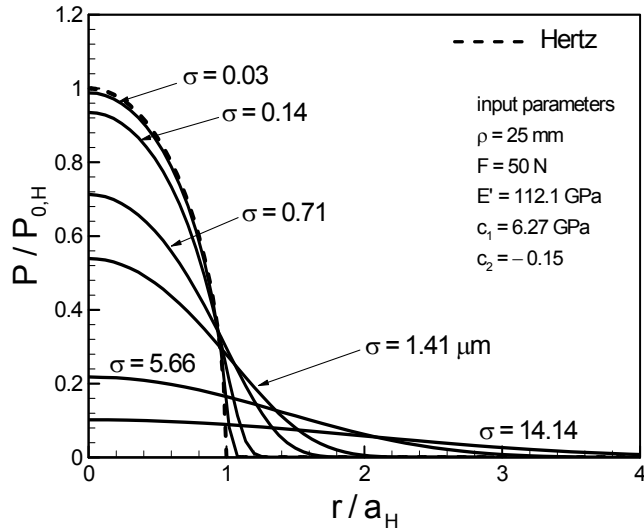


Figure 3. EFFECT OF ROUGHNESS ON PRESSURE DISTRIBUTION

the contact region and ii) the slope m is assumed to be a function of roughness σ .

Figure 4 illustrates several non-dimensional pressure distributions predicted by the model for some values of $P'_0 = P_0/P_{0,H}$ versus the non-dimensional radial location $\xi = r/a_L$. It was observed that the non-dimensional pressure distribution can be specified as a function of P'_0 and ξ . In other words, a general profile exists that covers all spherical rough contact pressures. The profile of the pressure distribution, especially in the contacts where P'_0 is less than 0.6, is very similar to a normal (Gaussian) distribution. However, as P'_0 approaches unity (the Hertzian contact) the pressure distribution profile begins to deviate from the normal profile. The general pressure distribution for spherical rough contacts was found to be

$$P(\xi) = P_0 (1 - \xi^2)^\gamma \quad (12)$$

where γ is calculated through a force balance to be

$$\gamma = 1.5 \frac{P_0}{P_{0,H}} \left(\frac{a_L}{a_H} \right)^2 - 1 \quad (13)$$

For the general pressure distribution, the relation between the maximum pressure P_0 and the applied force F is

$$P_0 = (1 + \gamma) \frac{F}{\pi a_L^2} \quad (14)$$

In the limit where roughness approaches zero, P'_0 and a'_L both approach unity, $\gamma = 0.5$, and Eqs. (12) and (14) yield the Hertzian pressure distribution, i.e., Eq. (2). With the

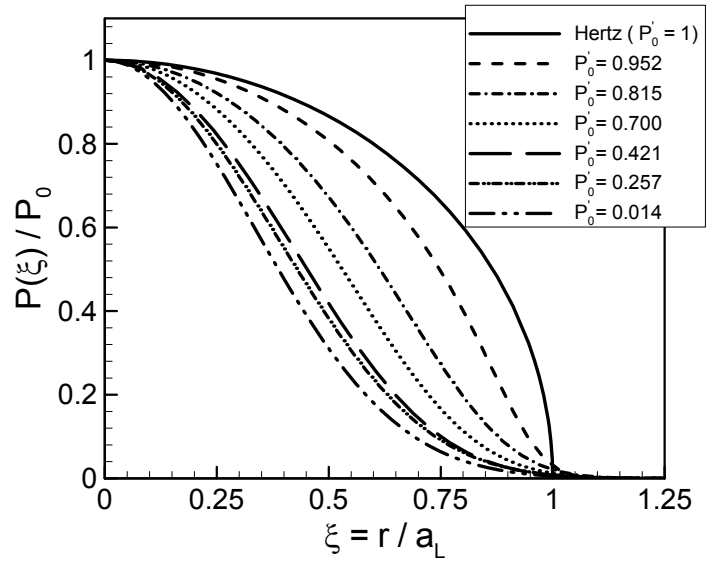


Figure 4. NON-DIMENSIONAL PRESSURE DISTRIBUTIONS FOR SPHERICAL ROUGH CONTACTS

Table 1. PHYSICAL INPUT PARAMETERS AND THEIR DIMENSIONS FOR SPHERICAL ROUGH CONTACTS

Parameter	Dimension
Effective elastic modulus, E'	$ML^{-1}T^{-2}$
Force, F	MLT^{-2}
Microhardness, H_{mic}	$ML^{-1}T^{-2}$
Radius of curvature, ρ	L
Roughness, σ	L
Max. contact pressure, P_0	$ML^{-1}T^{-2}$

general pressure distribution profile, i.e., Eq. (12), the problem is reduced to finding relationships for P_0 and a_L . Further, the radius of the contact area, based on its definition, can be found if P_0 and the pressure distribution are known, therefore the key parameter is the maximum contact pressure P_0 .

Dimensional analysis using the Buckingham II theorem has been applied to many physical phenomena such as fluid flow, heat transfer and stress and strain problems. The Buckingham II theorem proves that in a physical problem including n quantities in which there are m dimensions the quantities can be arranged into $n - m$ independent dimensionless parameters [18]. Table 1 summarizes the independent input parameters and their dimensions for spherical rough contacts. H_{mic} is an effective value for the micro-

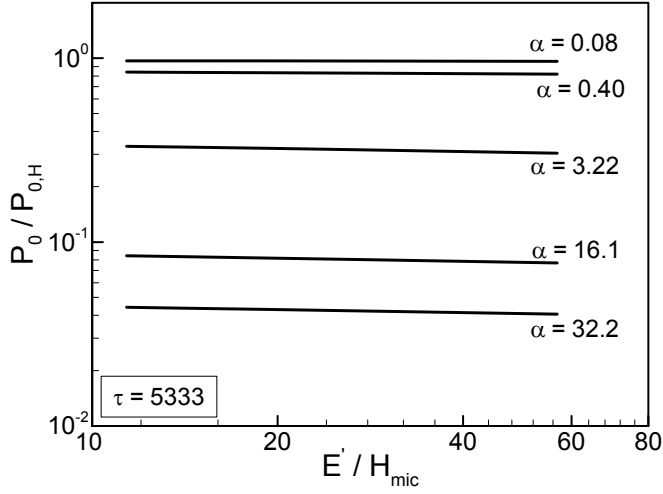


Figure 5. EFFECT OF MICROHARDNESS ON NON-DIMENSIONAL MAXIMUM CONTACT PRESSURE

hardness of the softer material in contact. The slope of asperities m may be estimated using an empirical relationship suggested by Lambert and Fletcher [19], $m = 0.076 \sigma^{0.52}$, where σ is the surface RMS roughness in micron. Therefore, the surface slope m is not considered as an independent input parameter. All quantities in Table 1 are known to be essential to the maximum contact pressure and hence some functional relation must exist in the form of

$$P_0 = P_0(\rho, \sigma, E', F, H_{mic}) \quad (15)$$

Applying the Buckingham II theorem there will be three II groups; so the maximum pressure can be more compactly stated as a function of these three non-dimensional parameters. Following Greenwood et al. [14], we chose the roughness parameter α . The other non-dimensional parameters are E'/H_{mic} and τ defined as

$$\tau = \frac{\rho}{a_H} = \left(\frac{4E'\rho^2}{3F} \right)^{1/3} \quad (16)$$

The present model described in the previous section was run for a wide range of input parameters to construct Figs. 5 - 7. As shown in Fig. 5, the effect of E'/H_{mic} on the maximum contact pressure is small and therefore ignored.

Figures 6 and 7 show P'_0 and a'_L as functions of α and τ over a wide range, respectively. As shown, P'_0 and a'_L are governed predominantly by the roughness parameter α and the other parameter τ has a minor role. As expected, as α decreases both P'_0 and a'_L approach unity, i.e., the Hertzian contact. The non-dimensional maximum contact pressure P'_0 and the contact radius a'_L were curve fitted and

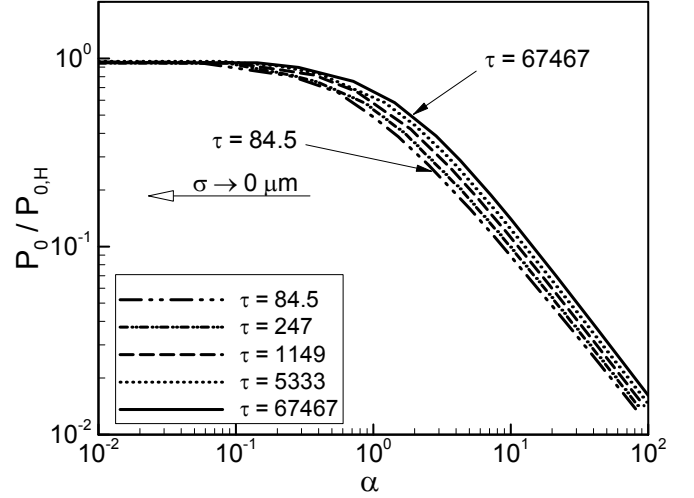


Figure 6. NON-DIMENSIONAL MAXIMUM CONTACT PRESSURE

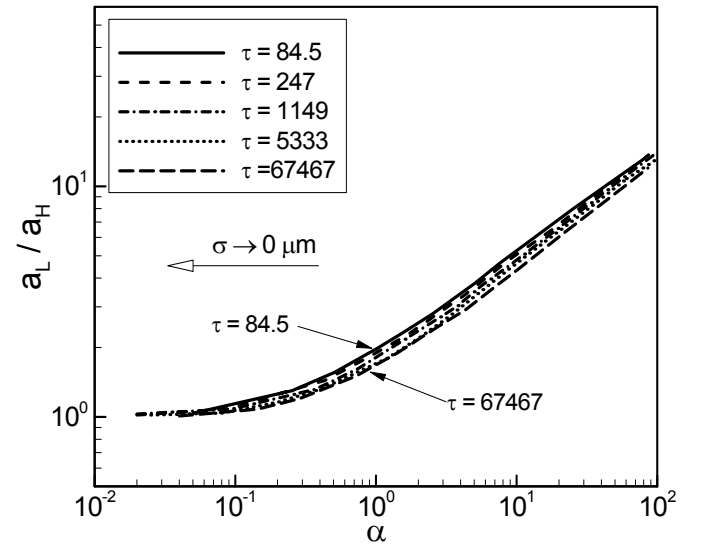


Figure 7. NON-DIMENSIONAL CONTACT RADIUS

the following expressions were found:

$$P'_0 = \frac{1}{1 + 1.37\alpha/\tau^{0.075}} \quad (17)$$

$$a'_L = \begin{cases} 1.605/\sqrt{P'_0} & 0.01 \leq P'_0 \leq 0.47 \\ 3.51 - 2.51P'_0 & 0.47 \leq P'_0 \leq 1 \end{cases} \quad (18)$$

The maximum difference between Eqs. (17) and (18) and the full model is estimated to be less than 4.5 percent in the range of $0.01 \leq P'_0 \leq 1$. Another relationship for the

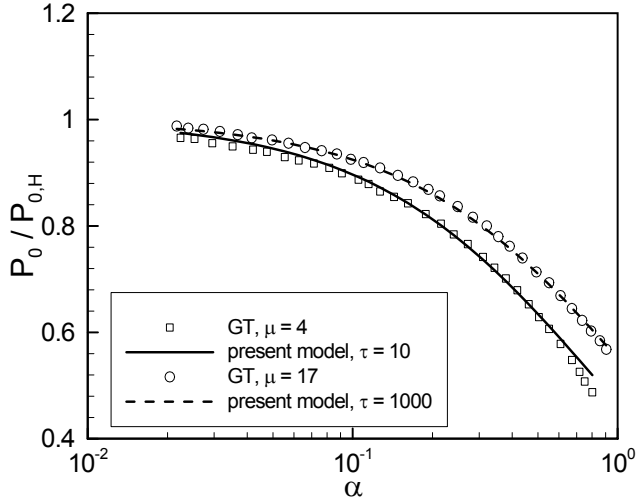


Figure 8. COMPARISON BETWEEN PRESENT MODEL AND GREENWOOD AND TRIPP MODEL

radius of the contact area was derived in the form of $a'_L = 1.80\sqrt{\alpha} + 0.31\tau^{0.056}/\tau^{0.028}$.

The maximum contact pressure P_0 from Eq. (17), is compared with the GT model in Fig. 8 over a range of α , for two values of μ which bracket a wide range of contacts [14]. As shown, both models demonstrate the same trend over the comparison range; the two values of τ were chosen to best fit the GT curves shown, they also cover a wide range of contacts.

COMPLIANCE

The elastic deformation of the half-space can be calculated by substituting the general pressure distribution Eq. (12) into Eq. (3), where the radius of the contact area is a_L :

$$\omega'_b(\xi) = \begin{cases} \frac{\pi}{4}B(0.5, \gamma + 1) & \xi = 0 \\ \int_0^\xi s(1-s^2)^\gamma K\left(\frac{s}{\xi}\right) ds & s < \xi \\ \int_\xi^1 (1-s^2)^\gamma K\left(\frac{\xi}{s}\right) ds & s > \xi \end{cases} \quad (19)$$

where $B(x, y)$ and $\omega'_b = \pi E' \omega_b / (4P_0 a_L)$ are the beta function and the non-dimensional bulk deformation, respectively. A general analytic solution for the integrals in Eq. (19) does not exist and they must be solved numerically for different values of γ . Since, the deformation at the edge of the contact area is required to calculate the compliance, Eq.

(19) was solved numerically for a wide range of γ at $\xi = 1$. The solution was correlated and the following relationship is proposed:

$$\omega_b(a_L) = \frac{4P_0 a_L}{\pi E' [4.79 - 3.17(P'_0)^{3.13}]} \quad (20)$$

where $0 < P'_0 \leq 1$. The maximum relative difference between Eq. (20) and the numerical solution is approximately 4.6 percent. In the Hertzian limit, elastic deformations of the half-space at the center and the edge of the contact area are:

$$\omega_{b,H}(0) = \frac{a_H^2}{\rho} = \frac{\pi P_{0,H} a_H}{2E'} \quad (21)$$

$$\omega_{b,H}(a_H) = \frac{a_H^2}{2\rho} = \frac{\pi P_{0,H} a_H}{4E'} \quad (22)$$

It can be seen that in the Hertzian limit, Eqs. (19) and (20) yield the Hertzian values, i.e., Eqs (21) and (22), respectively. Figure (9) shows non-dimensional deformations at the center $\omega'_b(0)$ and at the edge of the contact area $\omega'_b(a_L)$; in addition, the ratio of these deformations is shown in the plot over a wide range of P'_0 . As the non-dimensional maximum pressure decreases, i.e., the effect of roughness becomes more significant, bulk deformations at both the center and the edge of the contact decrease. As seen in Fig. (9), the ratio of deformations, $\omega_b(0)/\omega_b(a_L)$, increases as the non-dimensional maximum pressure P'_0 decreases. In other words, the ratio of $\omega_b(0)/\omega_b(a_L)$ is larger for “rougher” contacts which is a direct result of the general pressure distribution profile, i.e., the general pressure falls off faster than the Hertzian pressure, see Fig. (4).

The mutual approach of distant points in the two solids is called compliance. Compliance between rough spherical bodies is a function of asperity deformation $\omega_a(r)$, the bulk deformation $\omega_b(r)$, and the sphere profile and is given by $\kappa = r^2/2\rho + \omega_a(r) + \omega_b(r)$ [20]. Assuming the deformation of asperities at the edge of the contact area is zero $\omega_a(a_L) = 0$, the compliance can be found from

$$\kappa = a_L^2/2\rho + \omega_b(a_L) \quad (23)$$

Combining Eqs. (18), (20), and (23), one obtains

$$\kappa' = \frac{\kappa}{\kappa_H} = 0.5(a'_L)^2 + \frac{8P'_0 a'_L}{\pi^2 [4.79 - 3.17(P'_0)^{3.13}]} \quad (24)$$

where $\kappa_H = a_H^2/\rho$ is the Hertzian compliance. Equation (24) is plotted in Fig. (12) for a range of P'_0 .

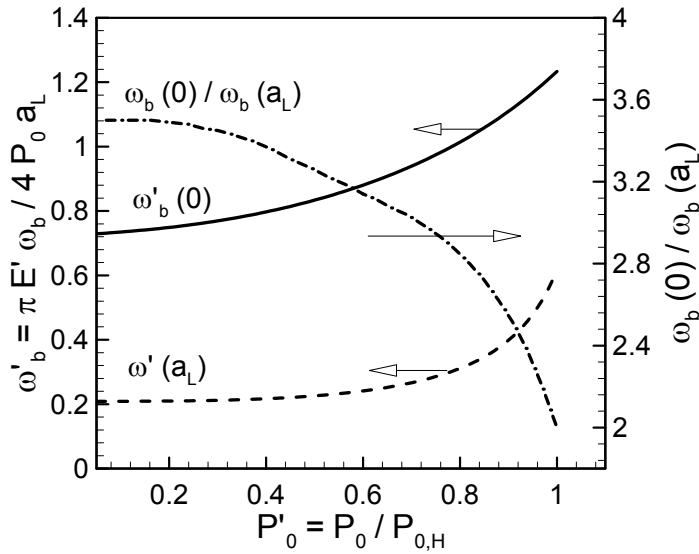


Figure 9. BULK DEFORMATION AT CENTER AND EDGE OF CONTACT AREA

COMPARISON WITH EXPERIMENTAL DATA

The results of the present model have been used in a thermal analysis to predict the thermal contact resistance (TCR) of spherical rough contacts in a vacuum. The developed model showed very good agreement with more than 280 experimental data points collected by many researchers during the last forty years [21]. Additionally, an analytical model has been developed to predict TCR of spherical rough surfaces in gaseous environments by the same authors using the general pressure distribution and very good agreement was observed with experimental data [22].

To verify the proposed model, the radius of the contact area and the compliance predicted by the model are compared with experimental data collected by Tsukada and Anno (TA) [23], Greenwood et al. (GJM) [14], and Kagami et al. (KYH) [20]. The experimental arrangement contains a smooth sphere placed in contact with a rough plane. The contact area was made visible by depositing a thin layer of copper [14] or an evaporated carbon film and a lamp black film [20]. The contact radii were measured using a metallographic microscope. Due to the measurement method, the experimental data may contain a relatively high uncertainty particularly at light loads or very rough surfaces since it involved some degree of judgment. Ranges of non-dimensional parameters α and τ covered by the experimental data are shown in Fig. 10. The experimental data include contact between similar (steel-steel) and dissimilar (steel-copper) materials and cover a relatively wide range of load, roughness, and radius of curvature. The proposed relationship for

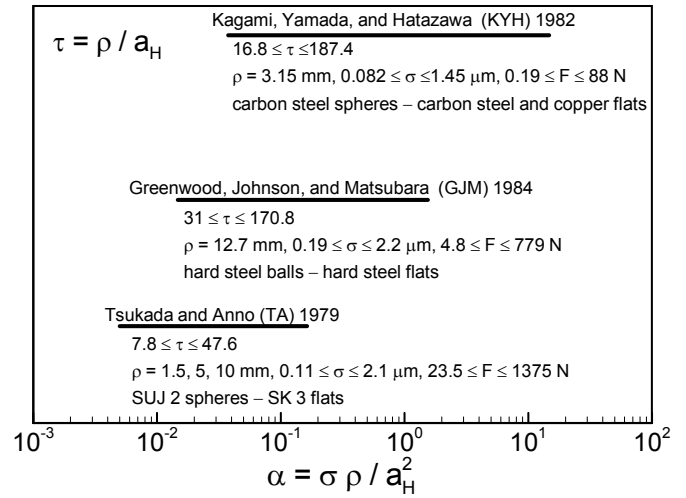


Figure 10. SUMMARY OF PARAMETER VALUES OF EXPERIMENTAL DATA

a_L , Eq. (18) is compared with the data in Fig. 11 and good agreement is observed. The present model shows the data trend over the entire range of the comparison. More than 160 data points, 26 sets, were compared with the present model in Fig. 11. Specimen materials, roughness, and radius of curvature for data sets are listed in Fig. 11. The RMS difference between the proposed expression and the data is approximately 6.2 percent.

Greenwood et al. [14] compared their data and Kagami et al. [20] data with the GT model. Their comparison showed a relatively high discrepancy especially with the Kagami et al. data. Greenwood et al. attributed the observed discrepancy to the experimental difficulties of measuring the contact radius. They also stated that the Kagami et al. data did not correlate particularly well with the roughness parameter α . However, as can be seen in Fig. 11, this discrepancy has not been encountered in this study. Additionally, our comparison shows that the Kagami et al. data (except for a few points for very rough surfaces at light loads) follow the correlation very well.

Kagami et al. [20] also measured the compliance between a smooth sphere and rough steel and copper plates. They collected more than 40 data points, two steel-steel and two steel-copper sets. Compliances were measured under various loads and with different roughness using differential transformers [20]. Figure 12 shows the comparison between the present model, Eq. (24) and the KYH compliance data. The present model shows good agreement with the RMS difference approximately 7.7 percent.

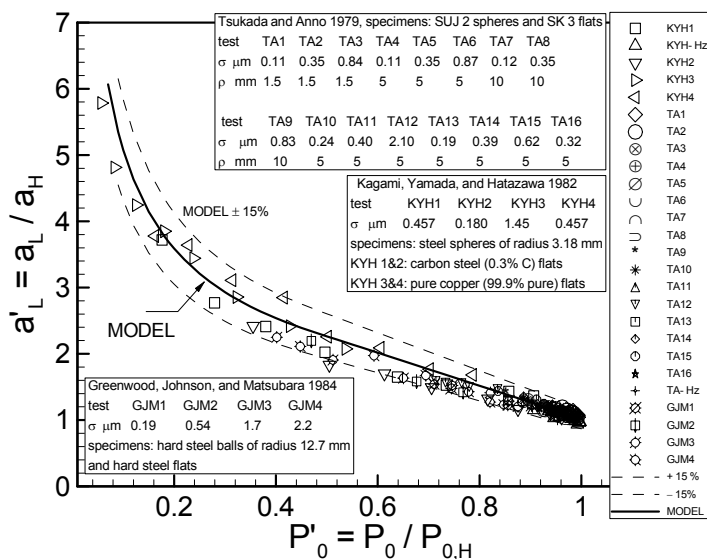


Figure 11. COMPARISON BETWEEN PRESENT MODEL AND EXPERIMENTAL DATA, CONTACT RADIUS

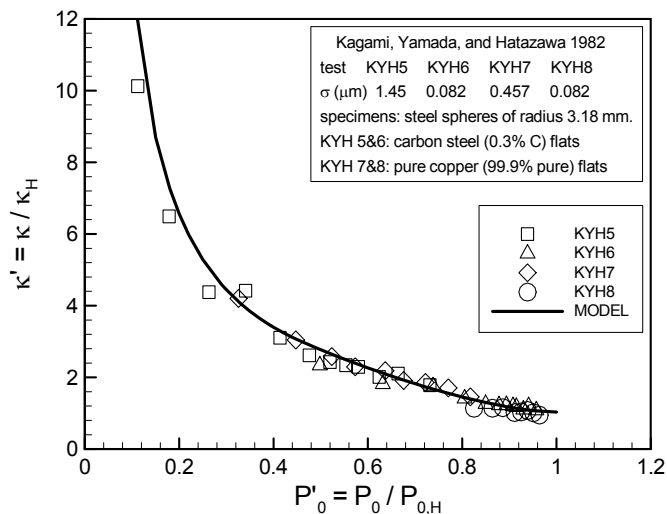


Figure 12. COMPARISON BETWEEN PRESENT MODEL AND EXPERIMENTAL DATA, COMPLIANCE

SUMMARY AND CONCLUSION

The mechanical contact of spherical rough surfaces was studied and a new model was developed. The deformations of surface asperities were considered to be plastic and the bulk deformation was assumed to be elastic. A closed set of governing relationships was derived and solved numerically. The pressure distributions predicted by the model

were plotted for different values of surface roughness and it was shown that as roughness approaches zero the predicted pressure distribution approached the Hertzian pressure.

A general pressure distribution was proposed that encompasses all spherical rough contacts. The maximum contact pressure was observed to be the key parameter that specifies the contact pressure distribution. The proposed general pressure distribution yields the Hertzian pressure at the limit where roughness was set to zero.

Using dimensional analysis, the number of independent non-dimensional parameters that describe the maximum contact pressure was determined to be three: $\alpha = \sigma\rho/a_H^2$, $\tau = \rho/a_H$, and E'/H_{mic} . The effect of the microhardness parameter E'/H_{mic} on the maximum contact pressure was observed to be small and therefore ignored. Using curve-fitting techniques, simple correlations were developed for calculating the maximum contact pressure and the radius of the contact area as functions of α and τ . Elastic deformation produced on the half-space as a result of applying the general pressure distribution was found. Compact relationships for the deformation at the center and at the edge of the contact area were proposed. Additionally, a simple expression for the compliance of spherical rough contacts was proposed.

The correlation proposed for the maximum contact pressure was compared with the GT model and a similar trend was observed. The compliance and the contact radius predicted by the model were compared against more than 200 experimental data points collected by others and showed good agreement.

ACKNOWLEDGMENT

The authors gratefully acknowledge the financial support of the Centre for Microelectronics Assembly and Packaging, CMAP and the Natural Sciences and Engineering Research Council of Canada, NSERC. Thanks go to Professor G. M. L. Gladwell for reading this paper and his comments.

REFERENCES

- [1] Williamson, J. B. P., Pullen, J. and Hunt, R. T., 1969, "The Shape of Solid Surfaces," Surface Mechanics, ASME, New York, pp. 24-35.
- [2] Cooper, M. G., Mikic, B. B., and Yovanovich, M. M., 1969, "Thermal Contact Conductance," Int. J. Heat Mass Transfer, Vol. 12, pp. 279-300.
- [3] Greenwood, J. A. and Williamson, B. P., 1966, "Contact of Nominally Flat Surfaces," Proc., Roy. Soc., London A295, pp. 300-319.

- [4] Chang, W. R., Etsion, I., and Bogy, D. B., 1987, "An Elastic-Plastic Model for the Contact of Rough Surfaces," *J. Tribology*, Vol. 109, pp. 257-253.
- [5] Zhao, Y., Maietta, D. M. and Chang, L., 2000, "An Asperity Microcontact Model Incorporating the Transition From Elastic Deformation to Fully Plastic Flow," *J. Tribology*, Vol. 122, pp. 86-93.
- [6] Tabor, D., 1951, *The Hardness of Metals*, Oxford, London, UK.
- [7] Johnson, K. L., 1985, *Contact Mechanics*, Cambridge University Press, Cambridge, UK.
- [8] Archard, J. F., 1953, "Contact and Rubbing of Flat Surfaces," *J. of Applied Physics*, Vol. 24, pp. 981.
- [9] Greenwood, J. A. and Wu, J. J., 2001, "Surface Roughness and Contact: An Apology," *Meccanica*, Kluwer Academic Publishers, 36, pp. 617-630.
- [10] Persson, B. N. J., 2000, *Sliding Friction Physical Principles and Applications*, Springer, Berlin, Germany.
- [11] Greenwood, J. A. and Tripp, J. H., 1967, "The Elastic Contact of Rough Spheres," *J. of Applied Mechanics*, Vol. 89, No.1, pp. 153-159.
- [12] Gladwell, G. M. L., 1980, *Contact Problems in the Classical Theory of Elasticity*, Alphen aan den Rijn: Sijthoff and Noordhoff, The Netherlands, Germantown, Maryland, USA.
- [13] Mikic, B. B. and Roca, R. T., 1974, "A Solution to the Contact of Two Rough Spherical Surfaces," *J. of Applied Mechanics*, ASME, 96, pp. 801-803.
- [14] Greenwood, J. A., Johnson, K. L., and Matsubara, E., 1984, "A Surface Roughness Parameter in Hertz Contact," *Wear*, 100, pp. 47-57.
- [15] Yovanovich, M. M. and Marotta, E. E., 2003, "Thermal Spreading and Contact Resistances," Chapter 4, *Heat Transfer Handbook*, Editors: A. Bejan and A. D. Kraus, John Wiley and Sons Inc, Hoboken, NJ, USA.
- [16] Hegazy, A. A., 1985, *Thermal Joint Conductance of Conforming Rough Surfaces: Effect of Surface Micro-Hardness Variation*. Ph.D. Thesis, Dept. of Mech. Eng., University of Waterloo, Waterloo, Canada.
- [17] Bahrami, M., 2004, *Modeling of Thermal Joint Resistance for Rough Sphere-Flat Contacts in a Vacuum*. Ph.D. Thesis, Dept. of Mech. Eng., University of Waterloo, Waterloo, Canada.
- [18] Streeter, V. L., and Wylie, E. B., 1975, *Fluid Mechanics*, McGraw-Hill Book Company, New York, USA.
- [19] Lambert, M. A. and Fletcher, L. S., 1997, "Thermal Contact Conductance of Spherical Rough Metals," *J. of Heat Transfer*, ASME, Vol. 119, Nov., pp. 684-690.
- [20] Kagami, Y., Yamada, K., and Hatazawa, T., 1982, "Contact Between a Sphere and Rough Plates," *Wear*, 87, May, pp. 93-105.
- [21] Bahrami, M., Culham, J. R., and Yovanovich, M. M., 2003, "A Scale Analysis Approach to Thermal Contact Resistance," ASME International Mechanical Engineering Congress, Nov. 15-21, Washington D.C., USA, Paper No. IMECE2003-44097.
- [22] Bahrami, M., Culham, J. R., and Yovanovich, M. M., 2003, "Thermal Resistance of Gaseous Gap for Non-Conforming Rough Contacts," 42nd AIAA Aerospace Meeting and Exhibit, Jan. 5- 8, Reno, Nevada, USA, Paper No. AIAA2004-0822.
- [23] Tsukada, T. and Anno, Y., 1979, "On the Approach Between a Sphere and a Rough Surface (1st. Report-Analysis of Contact Radius and Interface Pressure," (in Japanese), *J. of the Japanese Society of Precision Engineering*, Vol. 45, No. 4, pp. 473-479.